Integrating core and log data in the petrophysical rock type approach to identify flow units and predict permeability in a carbonate reservoir of Campos Basin

Heitor Lichotti & Abel Carrasquilla, UENF/LENEP, Macaé – RJ

Abstract

This work characterizes the carbonate reservoir of Field A, located in the Campos Basin, using wireline logs and laboratory petrophysical data. The marked variation of petrophysical properties, a characteristic inherent to carbonate reservoirs, is a motivating factor for this work, which seeks to overcome the difficulties of this evaluation. In this sense, this work proposes to divide the reservoir region into zones in accord to different petrophysical characterization models, such as lithofacies descriptions, petrophysical zones, units and flow zones. Dataset from two wells in the oilfield was then interpreted, from which petrophysical parameters such as porosity and permeability were derived with a good correlation coefficient with the core laboratory data. The multiple linear regression, the Cluster Analysis for Rock Typing and Hydrodynamic Flow Unit modules of the Interactive Petrophysics – IP (Senergy, 2016) software were utilized, to evaluate the Reservoir Quality Index, the Flow Zones and Hydraulic Flow Units. Once these petrophysical characteristics of the first well (A03) were determined, a blind test and a correlation with the second well (A10) were performed. With this methodology, it was possible to predict the potential zones and, thus, to provide information that feed geological models that simulate the behavior of the reservoir in production.

Introduction

In this work, a study of flow zoning of the carbonate reservoir of Field A of the Campos Basin was built up. From this, it was proposed a method for determining permeability by combining linear regressions in accord to the flow units in which this part of the reservoir is contained. Eventually, it validates the models developed against experimental data of porosity and permeability of oil reservoir rocks. This integration of well log data and laboratory petrophysical data can therefore bring forth solutions that lead to the exploration and production of oil in carbonate reserves and provide a basis for a methodology and workflow for similar reservoirs.

Most of the hydrocarbon reservoir in the world is located in carbonate rocks. Regarding Lucia (2007), carbonates cover about 7% of the Earth's surface, even so, more than 60% of the world's oil reserves and 40% of gas are present in them, of which 70% corresponds to the giant fields of Middle East. These carbonate reservoirs are still subjected to an intense diagenetic process, which may include cementation, dissolution, dolomitization, recrystallization and biogenic action. The lithological complexity resulting from these processes makes it difficult to characterize these rocks, when compared to siliciclastic ones. The Campos Basin is the largest oil producer in the Brazilian continental margin, currently accounting for more than 70% of the national production. The oilfields present in this basin include Albian carbonate reservoirs, with averages of porosity and permeability of 25% and 250 mD, respectively. Given the complex heterogeneity of carbonate reservoirs, normally it exists a low recovery factor, and a difficult correlation between rock properties and geophysical data. The characterization of carbonate reservoirs through an integrated study between their petrophysical properties and their well logs provides a fundamental understanding of their geometry and their dynamic properties (Bruhn et al., 2003).

The integration of geological and petrophysical data allows the development of a rock - fluid model for the reservoirs. This type of study identifies the different types of rocks that make up the reservoirs, as well as those non-reservoirs. A PRT (Petrophysical Rock Types) is defined as a rock interval with singular pore geometry, a certain mineralogical composition and with certain specific characteristics of fluid flow. The fluid rock model relates fluid flow characteristics to certain PRT, using analytical techniques to develop such a model as the porosity and permeability analysis of the samples, plugs gas permeability measurements, thin sheet analysis, analysis of electron microscope pore structures, capillary pressure by mercury injection, pore throat size distribution and the interpretation of well logs. The consolidation of the results of these various analysis techniques reveals the existence of lithofacies, and it is hoped that similarities between the models proposed by the various techniques will result (Amaefule et al., 1993).

The classification of the reservoir rock, in accord to Amaefule et al. (1993), is a synergistic process between geology, petrophysics and reservoir engineering, through which a reservoir volume is divided into a limited number of rock types that have:

a) Different ranges of petrophysical properties (porosity, permeability, water saturation and capillary pressure characteristics) or distinct correlations between the fundamental properties.
b) Common diagenetic features, including both depositional facies and diagenesis, which determined pore types and geometries present, and thus the petrophysical properties.

The geological qualification thus allows the PRT, and therefore the petrophysical properties, to be distributed in a three-dimensional reservoir model based on a deposition model and stratigraphic sequences together with the understanding of the diagenetic processes controlling Changes in reservoir quality (Al-Tooqi et al., 2014). Published examples of PRT fall into two general broad categories. PRT performed by petrophysicists as demonstrated by Gomaa et al. (2006) and Jooybari et al. (2010) typically shows clear differentiation between groups of samples in terms of petrophysical parameters (porosity, permeability, flow zone indicator and other measurements related to reservoir performance permeability). However, these groups tend to be weakly linked to a structural geology, in such a way that the three-dimensional distribution of the defined PRT is highly ambiguous. On the other hand, the PRT carried out by geologists, like the one carried out by Hollis et al. (2010), is commonly based on lithofacies groupings combined with one or two diagenetic modifiers. This results in a clear relationship in a chronostratigraphic three-dimensional deposition model, but with a PRT that may have broadly variable and highly overlapping ranges of petrophysical properties. Skalinski and Kenter (2015) recently reviewed the many challenges and disruptions involved in PRT, and proposed a comprehensive workflow to address these matters.

Method

The dataset used in this work includes well logs (gamma rays, resistivity, density, neutron and sonic) and laboratory basic petrophysical data (porosity and permeability) for wells A3 and A10 drilled in the Field A in the Campos Basin. These wells were selected for their physical proximity and for the similarity of the log data, which indicate that the rocks of both wells have similar characteristics, composed mainly of a fine grainstone, hairy carbonate rock with oncoliths and cemented with calcite.

The methodology of this study initially consists of working the available dataset in the commercial software IP (Senergy, 2016) and to explore the different interpretation modules that it offers for preliminary petrophysical characterization (porosity, permeability, saturation of fluids, etc.). Afterwards, the PRT concept will be applied, as well as the comparison between their different models, and finally the determination of the best method to estimate the permeability, aiming at the wider characterization of the reservoir. IP software also includes a module called "Hydraulic Flow Units" (HFU) that, from the porosity and permeability data, allows the distribution of the reservoir in flow units through the following approaches: Reservoir Quality Index (RQI) and Winland - Pitman Method (Winland, 1972; Pitman, 1992). The module allows the selection of the porosity and permeability curves that will be taken as input for the determination of flow units.

Results

In the porosity v's permeability graph (Figure 1) of the R35 curves of Winland (1972) for wells A03 (a) and A10 (b), we can observe a pore grouping that matches the facies identification proposed by Petrobras () in the analysis of Group 1 (green) referring to megapores, with pore sizes <10μm, there is a predominance of cemented grains. In Group 2 (yellow), we have the macropores with a slightly smaller pore size, ranging from 2 - 10 mm, and in this group we still observe some points referring to the cementless grainstones, but also identifies the marked presence of packstones. In Group 3, blue, are located Mesopores, with pore sizes ranging from 0.5 - 2 mm, in this group the dominant lithology is the packtones with presence of cemented packtones, wackstones and a few grainstones. Finally, in Group 4, the micropores, with a pore size of less than 0.5 mm, are present all the lithologies identified by Petrobras (2012), with a higher percentage of points being related to packstones, cemented packstones and wackstones.

In the HFU module of IP, we first select the well and the curves that governed the calculations for determining the flow units. For well A03, the selection of the porosity curve was performed first, as the results of the laboratory analysis and we do the same for the permeability. Then we select the number of flow units desired for the modeling. Such number was previously determined through the SMLP (Stratigraphic Modified Lorenz Plot), not shown in this article. For both wells the number of flow units in conformity to the SMLP, was 8 flow units. The choice of the margins for determining the clustering of points in each flow unit is computed automatically by the IP, through cluster analysis. The curves of RQI ($RQI = 0.0314\sqrt{(k/\phi_e)}$, k being the permeability and ϕ_e the effective porosity), ϕ_Z (pore volume - to - grain volume ratio, $\phi_Z = \phi_e/(1 - \phi_e)$,) and FZI (Flow Zone Indicators, $FZI = RQI/\phi_Z$) are computed automatically by the IP that still calculates the permeability equations for each of the flow units, previously determined (Amaefule et al., 1993).

For well A03, the FZI values of the plugs range from 0,071 a 259,67. In order to obtain measurements that best represent the HFU of the reservoir, the plugs that presented near FZI were grouped in the same HFU, according to the limits defined with the module cluster analysis as shown in Figure 3a. The IP Software, through the module HFU, elaborates, using a linear regression, the permeability equations for each of the previously defined flow units, and calculates the correlation factor R^2 for each of the proposed equations. The equations for each of the HFU are shown Figure 3b. The graph with the ϕ_Z vs RQI distribution is shown in Figure 3c. For well A10, the FZI values of the plugs range from 0.1405 to 21.1688. In order to obtain measurements that best represent the HFU of the reservoir, the plugs that presented near FZI were grouped in the same HFU, according to the limits defined with the module cluster analysis as shown in Figure 4a. The IP Software, through the HFU module, elaborates, using a linear regression, the permeability equations for each of the previously defined flow units, and calculates the correlation factor R^2 for each of the proposed equations. The equations for each of the HFU are shown Figure 4b. The graph with the ϕ_Z vs RQI, on the other hand, distribution is shown in Figure 4c.

In Figure 5a, we can observe in the track 6 (Permeability 1) the permeability estimation by the RQI methodology calculated on the laboratory porosity, and in track 7 Permeability by the RQI methodology calculated on the sonic porosity, in black we have the results of the laboratory measurements on the plugs. It is also observed that these

permeability curves, both the permeability from the laboratory porosity and the permeability from the sonic log, present both excellent behavior when compared to the permeability measured in the laboratory which indicates that the model of flow units, it was very consistent in the case studied. The permeability estimation based on the laboratory porosity data, adjusted in accord to the RQI model, presented very good results, with a correlation factor R^2 = 89.99 %. The permeability estimation based on the sonic porosity data, adjusted in accord to the RQI model, also presented good results, with a correlation factor R^2 = 88.55 %. Figure 5b is a plot generated in the IP, with the permeability curves generated by the two models mentioned above, compared with the laboratory measurements and with the facies models, flow zones and flow units for the Well A10. As occurred in well A03, in well A10 the permeability model from the equations for the flow units again is very consistent.

In an effort to better understand the carbonate reservoir through the two wells analyzed, we looked for ways to correlate the identified zones in well A03 and A10. Foremost, the flow zones determined for each well were analyzed in the reservoir region in a try to find a corresponding pattern (Figure 6a). In a second moment, the correspondences between the conventional logs are examined. We discovered that the gamma, density, neutron and sonic logs presented the same pattern of behavior in the two wells studied, confirming the correlations between the previously correlated flow units (Figure 6b).

Conclusions

The permeabilities calculated by modeling the values of the laboratory porosities and the sonic log presented both excellent correlations with the permeability measured in the laboratory. This shows the efficiency of the reservoir division method in flow units, which allowed the elaboration of different equations to calculate the permeability, as a function of the porosity, for each of the HFU previously defined. These individualized equations were later combined in a single equation that interpolates values according to the RQI, to the depth, resulting in a correlation factor of more than 90% in both analyzed porosities. Permeability from sonic porosity could then be applied to both wells to predict permeability in the untested regions from the RQI analysis. This fact gives indications of its applicability and extrapolation of these results in other wells in the field studied. From the correlation of the two studied wells, we can deduce that the zones and flow units present in A3 are all identified also in A10. However, in the latter well they are displaced to a higher region, about 30m high, which Suggests A10 was drilled in a region on a structural top, in a more central position of the reservoir. The potentially more productive zones indicated for the two wells have all predominance of lithofacies of uncemented grains with pore throat radius classified as mega or macropores. This gives good permoporous characteristics to these zones, which is compatible with the RQI analysis, elaborated for the same sites. The integration of petrophysical, geophysical and geological data helped to better infer the properties of the reservoir. It was observed that the location of the wells influences the quality of the reservoir rock that it crosses and the final productivity of each well.

Acknowledgments

We thank UENF/LENEP for the computational infrastructure and Petrobras by the dataset.

References

- Amaefule, J.; Altunbay, M.; Tiab, D.; Kersey, D. & Keelan, D. 1993. Enhanced reservoir description: using core and log data to identify hydraulic flow units and predict permeability in uncored intervals/wells. SPE Annual Technical Conference and Exhibition, Housto, p. 205 - 220.
- Al-Tooqi, S.; Ehrenberg, S.; Al-Habsi, N.; Al-Shukaili, M. 2014. Reservoir rock typing of upper Shu Aiba limestones, northwestern Oman. Petroleum Geoscience, v. 20, n. 4, p. 339 -352.
- Bruhn,C.; Gomes, J.; Lucchese Jr., C. & Johann, P. 2003. Campos Basin: reservoir characterization and management - historical overview and future challenges. Offshore Technology Conference. OTC 15220.
- Gomes, J; Ribeiro, M.; Strohmenger, C.; Naghban, S. & Kalam, M. 2008. Carbonate reservoir rock typing - the link between geology and scal. SPE Abu Dhabi International Petroleum Exhibition and Conference, Paper 118284-MS.
- Gomaa, N.; Azer, S.; Ouzzane, D.; Saif, O.; Okuyiga, M.; Allen, D.; Rose, D.; Ramamoorthy, R. & Bize, E. 2006. Case study of permeability, vug quantification, and rock typing in a complex carbonate. SPE Annual Technical Conference and Exhibition, Santo Antonio, paper 102888- MS.
- Hollis, C.; Vahrenkamp, V.; Tull, S.; Mookerjee, A.; Taberner, C. & Huang, Y. 2010. Pore system characterisation in heterogeneous carbonates: an alternative approach to widely - used rock - typing methodologies. Marine and Petroleum Geology, v. 27, n. 4, p. 772 - 793.
- Jooybari, H.; Movazi, G. & Jaberi, R. 2010. A new approach for rock typing used in one of the Iranian carbonate reservoir (a case study). SPE International Oil and Gas Conference and Exhibition, Beijing, paper 131915-MS.
- Lucia, J. 2007. Carbonate reservoir characterization: an integrated approach. Springer - Verlag Berlin Heildelberg, 343 p.
- Petrobras. 2012. UENF / Petrobras Cooperation Agreement.
- Pittman, E. 1992, Relationship of porosity to permeability to various parameters derived from mercury injection - capillary pressure curves for sandstone. AAPG Bulletin, v. 76, n. 2, p. 191 - 198.
- Skalinski, M. & Kenter, J. 2015. Carbonate petrophysical rock typing: integrating geological attributes and petrophysical properties while linking with dynamic behaviour. Special Publications, Geological Society, London, v. 406, n. 1, p. 229–259.
- Senergy. 2015. Interactive Petrophysics Software. User´s Manual.
- Winland, H. 1972. Oil accumulation in response to pore size changes, Weyburn field, Saskatchewan: Amoco Production Company. Report F72-G-25, 20 p.

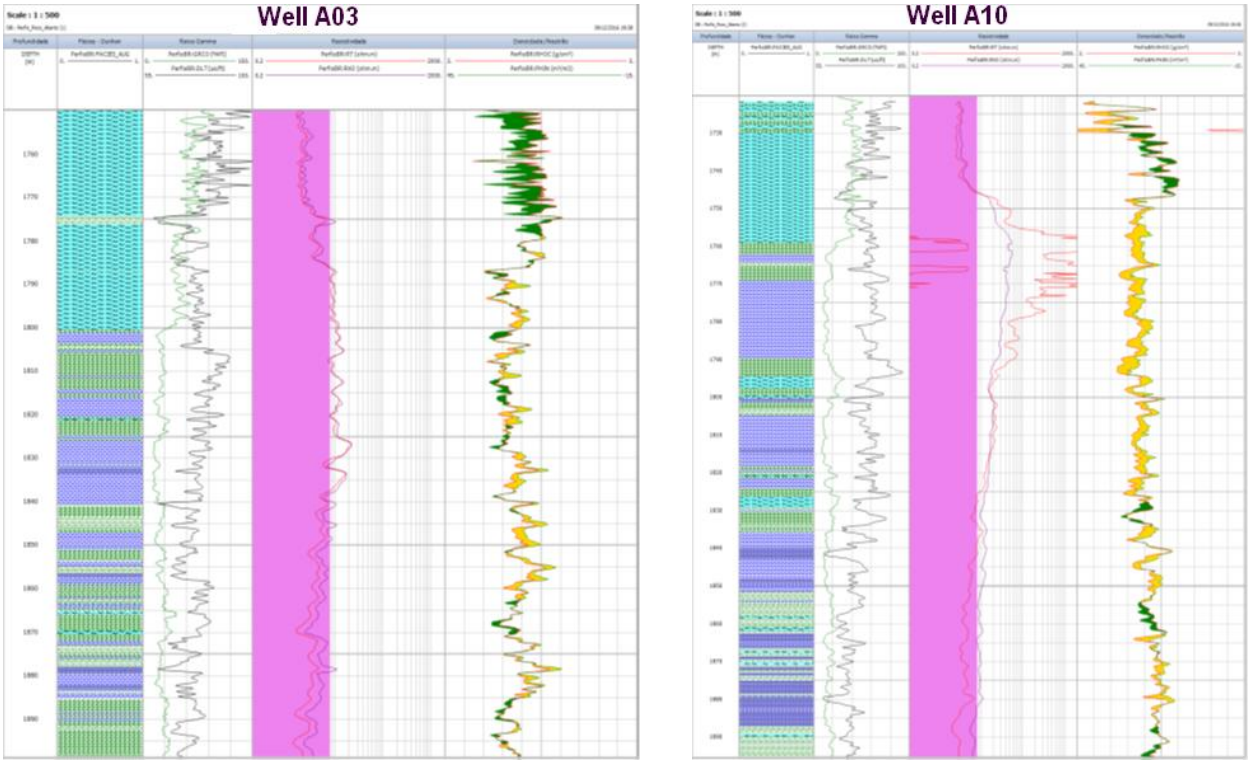

Figure 1. Lithofacies (track 2) and basic logs of wells A03 and A10: gamma ray and transit time logs (track 3), resistivity logs (track 4) and density and neutron porosity (track 5) for wells A03 e A10.

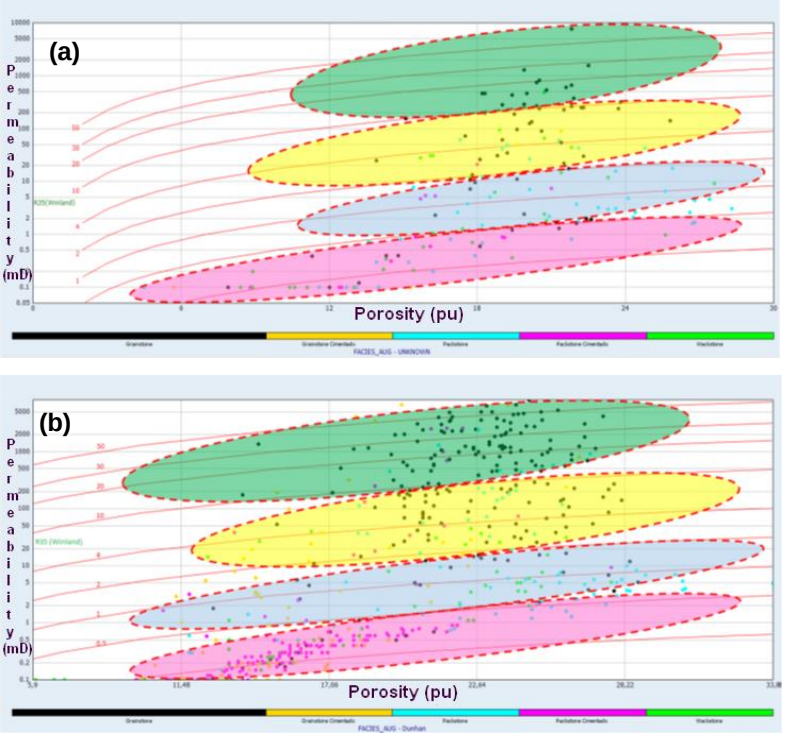

Figure 2. Distribution of pore sizes with Winland (1972) R35 curves for wells A03 (a) and A10 (b): green (≥ 10μm), yellow (2 - 10 μm), blue light (0.5 - 2 μm) and pink (<0.5 μm), corresponding to, respectively, mega (grainstones), macro (not cimented grainstones and packstones), meso (cimented packstones, wackstones and few grainstones) and micro (packstones, cimentes packstones and wackstones) pores.

(a)

HFU	FZI (intervals)
1	0,1405 - 0,252
2	0,252 - 0,380
3	0,380 - 0,532
4	0,532 - 0,873
5	0,873 - 1,494
6	1,494 - 3,080
7	3,080 - 6,656
8	6,656 - 21,1688

(b)

HFU	Permeability Equations	R^2 (%)
1	$k = \phi^3.(0,199/(0,0314(1-\phi)))^2$	92,59
2	$k = \phi^3.(0,310/(0,0314(1-\phi)))^2$	96,21
3	$k = \phi^3.(0,430/(0,0314(1-\phi)))^2$	98,68
4	$k = \phi^3.(0,708/(0,0314(1-\phi)))^2$	97,92
5	$k = \phi^3.(1,100/(0,0314(1-\phi)))^2$	95,32
6	$k = \phi^3.(2,143/(0,0314(1-\phi)))^2$	34,05
7	$k = \phi^3.(4,544/(0,0314(1-\phi)))^2$	35,87
8	$k = \phi^3.(9,203/(0,0314(1-\phi)))^2$	35,18

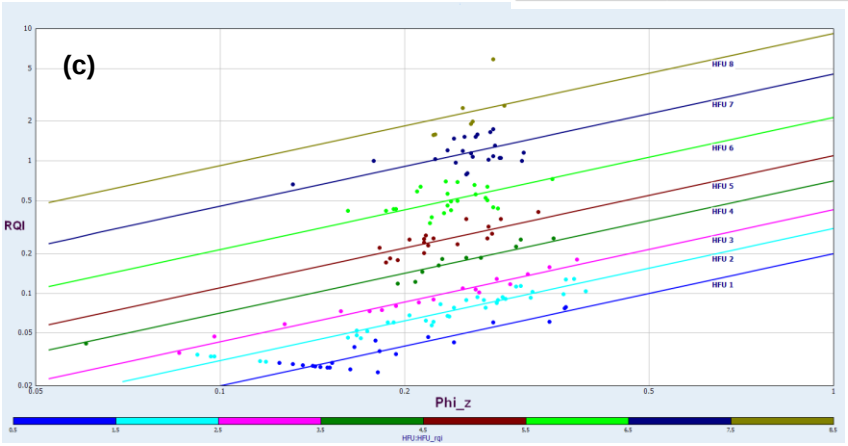

Figure 3. Well A03: (a) Flow units and ranges of corresponding IZF values. (B) Equations for permeability based on laboratory porosity - UFs. (C) Distribution ϕ_z versus RQI (calculated for laboratory porosity).

(a)

HFU	FZI (intervals)
1	0,071 - 0,252
2	0,252 - 0,383
3	0,383 - 0,666
4	0,666 - 2,135
5	2,135 - 4,776
6	4,776 - 7,886
7	7,886 - 18,00
8	18,00 - 259,676

(b)

HFU	Permeability Equations	R^2 (%)
1	$k = \phi^3.(0,229/(0,0314(1-\phi)))^2$	90.27
2	$k = \phi^3.(0,428/(0,0314(1-\phi)))^2$	95.12
3	$k = \phi^3.(0,751/(0,0314(1-\phi)))^2$	95.51
4	$k = \phi^3.(1,313/(0,0314(1-\phi)))^2$	93.04
5	$k = \phi^3.(2,181/(0,0314(1-\phi)))^2$	83.84
6	$k = \phi^3.(3,873/(0,0314(1-\phi)))^2$	64.92
7	$k = \phi^3.(6,680/(0,0314(1-\phi)))^2$	79.55
8	$k = \phi^3.(13,025/(0,0314(1-\phi)))^2$	7.470

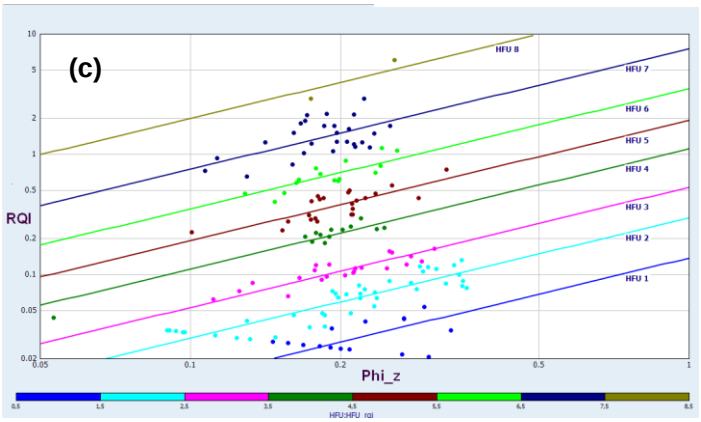

Figure 4. Well A10: (a) Flow units and ranges of corresponding IZF values. (B) Equations for permeability based on laboratory porosity - UFs. (C) Distribution ϕ_z versus RQI (calculated for laboratory porosity).

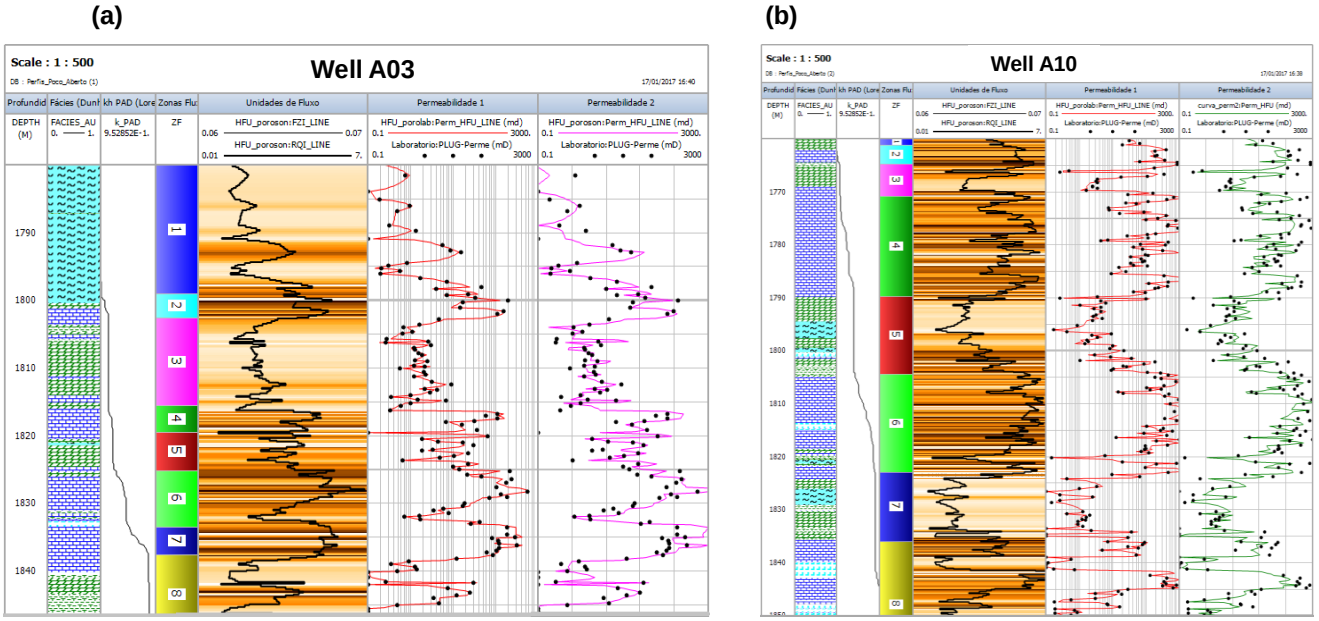

Figure 5. Lithofacies (track 2), Lorenz curve (track 3), flow zones (track 4), flow units (track 5), permeability curves for wells A03 (a) and A10 (b), compared with laboratory measurements (tracks 6 and 7).

based on laboratory porosity - UFS. (C) Distribution ϕ_z versus RQI (calculated for laboratory porosity).

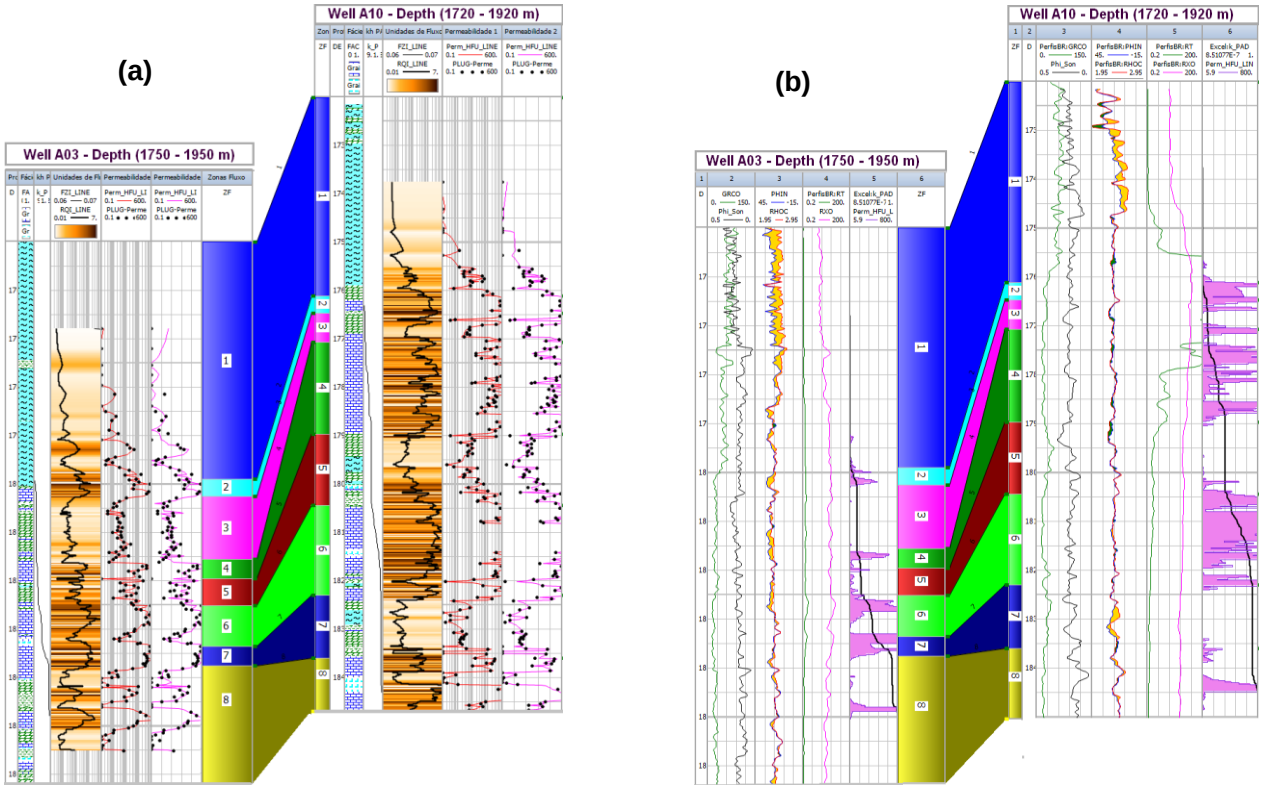

Figure 6. Comparative between the flow zones (a) and between the basic well logs (b) of the wells A03 and A10.